Carbon assimilation in *Eucalyptus urophylla* grown under high atmospheric CO$_2$ concentrations: A proteomics perspective

Bruna Marques dos Santos, Tiago Santana Balbuena *

Departamento de Tecnologia, Faculdade de Ciências Agrárias e Veterinárias, Universidade Estadual "Júlio de Mesquita Filho", Jaboticabal, SP, Brazil

ABSTRACT

Photosynthetic organisms may be drastically affected by the future climate projections of a considerable increase in CO$_2$ concentrations. Growth under a high concentration of CO$_2$ could stimulate carbon assimilation—especially in C3-type plants. We used a proteomics approach to test the hypothesis of an increase in the abundance of the enzymes involved in carbon assimilation in *Eucalyptus urophylla* plants grown under conditions of high atmospheric CO$_2$. Our strategy allowed the profiling of all Calvin-Benson cycle enzymes and associated protein species. Among the 816 isolated proteins, those involved in carbon fixation were found to be the most abundant ones. An increase in the abundance of six key enzymes out of the eleven core enzymes involved in carbon fixation was detected in plants grown at a high CO$_2$ concentration. Proteome changes were corroborated by the detection of a decrease in the stomatal aperture and in the vascular bundle area in *Eucalyptus urophylla* plantlets grown in an environment of high atmospheric CO$_2$. Our proteomics approach indicates a positive metabolic response regarding carbon fixation in a CO$_2$-enriched atmosphere. The slight but significant increase in the abundance of the Calvin enzymes suggests that stomatal closure did not prevent an increase in the carbon assimilation rates.

Biological significance: The sample enrichment strategy and data analysis used here enabled the identification of all enzymes and most protein isoforms involved in the Calvin-Benson-Bessham cycle in *Eucalyptus urophylla*. Upon growth in CO$_2$-enriched chambers, *Eucalyptus urophylla* plantlets responded by reducing the vascular bundle area and stomatal aperture size and by increasing the abundance of six of the eleven core enzymes involved in carbon fixation. Our proteome approach provides an estimate on how a commercially important C3-type plant would respond to an increase in CO$_2$ concentrations. Additionally, confirmation at the protein level of the predicted genes involved in carbon assimilation may be used in plant transformation strategies aiming to increase plant adaptability to climate changes or to increase plant productivity.

1. Introduction

Photosynthesis is a multi-step cellular process that converts atmospheric CO$_2$ into triose-phosphate sugars. According to the NOAA Global Monitoring Division [1], Earth's average atmospheric CO$_2$ concentration reached the 400-ppm milestone in 2016, the highest recorded concentration since monitoring began at the Mauna Loa Observatory in 1958 [2]. Current projections estimate that global CO$_2$ concentration will continuously rise in the near future and that in the worst case scenario, it will reach a concentration equal to 985 ppm by 2100 (RCP8.8 at [3]). Of all photosynthetic organisms, the metabolism of C3-type plants may be more severely affected by this new atmospheric scenario; CO$_2$ competes with oxygen at the active site of the enzyme RuBisCO, which is a key player in the first step of carbon fixation into organic molecules.

Carbon assimilation is driven by tandem and parallel reactions of 11 enzymes in the chloroplast stroma; most of these enzymes are encoded by the plant nuclear genome, and only one is encoded by the plastid genome. In *Arabidopsis thaliana*, 36 gene products are directly involved in the carbon fixation process [4], while the recently sequenced *Eucalyptus grandis* genome indicated a higher genome redundancy, with at least 46 gene products directly involved in the carbon fixation cycle [5]. Due to their central role in the primary metabolism of plants, these enzymes are usually abundant and therefore easy to target by large-scale protein studies that cannot make use of amplification steps that are usually adopted by transcript-level approaches.

Proteomics has the capacity to identify and quantify hundreds to thousands of gene-related products. Sub-cellular proteomics is a field that targets a specific cellular compartment and the biochemical processes that occur within it. Regular workflows make use of organelle-enrichment steps to reduce the proteome sample complexity and consequently, to increase the sensitivity of the analysis [6–7]. In one of

---

* Corresponding author at: Departamento de Tecnologia, Universidade Estadual Paulista "Júlio de Mesquita Filho", Via de Acesso Prof Paulo Donato Castellane, 14884-900 Jaboticabal, SP, Brazil.

E-mail address: tsbalbuena@fcav.unesp.br (T.S. Balbuena).

the first attempts to carry out a plastid proteome analysis, a total of 690 proteins were confidently identified from purified *Arabidopsis thaliana* chloroplasts [8]. This pioneering work paved the way for subsequent sub-cellular proteomics approaches in different plant organisms and showed the potential of the strategy to elucidate metabolic regulation taking place in and between cellular organelles.

Eucalyptus sp. are C3-type plants that are extensively used as major natural sources for the production of pulp, paper, biomaterials and energy [9]. Wullschleger et al. [10] and Atwell et al. [11] suggested that *Eucalyptus* plants are among the woody plants that are the most sensitive to an increase in CO_2 concentrations. A recent study reported a significant enhancement of photosynthesis and growth in *Eucalyptus globulus* plants cultivated in an atmosphere of enriched CO_2 [12]. Here, we investigated the *Eucalyptus urophylla* chloroplastic proteome in order to evaluate whether the abundance of the eleven Calvin-Benson cycle enzymes involved in carbon fixation would be affected by growth in high concentrations of atmospheric CO_2.

2. Materials and methods

2.1. Plant material and growth conditions

Clonal seedlings of *Eucalyptus urophylla* were acquired in a local nursery and grown in controlled environment chambers with the temperature adjusted to 27 °C, photon flux density at 187 μmol m^{-2} and a 12 h day/night cycle. Atmospheric CO_2 concentrations inside the growth chambers were adjusted to 400 ppm and 1000 ppm for the control and treated plants, respectively. After 10 weeks of growth, young leaves were harvested and immediately subjected to chloroplast isolation and microscopy analysis. Three biological replicates were used for chloroplast isolation and stomatal aperture evaluation, while four and six biological replicates were used in the leaf anatomy and chlorophyll fluorescence analyses, respectively.

2.2. Chloroplast isolation

Chloroplast isolation was carried out according to the Sigma-Aldrich Chloroplast Isolation Kit protocol. An aliquot of 3 g of leaves was collected, washed and kept on ice. Then, the midrib was removed, and leaves were cut into small pieces prior to being transferred to 18 mL of cold chloroplast isolation buffer (CIB) containing 0.1% BSA. After homogenization, leaf material was filtered on a nylon membrane and centrifuged at 200 ×g for 3 min at 4 °C. From the collected supernatant, chloroplasts were precipitated by centrifugation at 1000 ×g for 7 min (4 °C) and resuspended in 1 mL of CIB containing 0.1% BSA. Chloroplasts were then purified by discontinuous Percoll density gradient centrifugation (80/40%, 1:2) at 3200 ×g for 15 min at 4 °C. Intact chloroplasts in the Percoll interface were collected and transferred to a clean tube. Finally, two wash steps were carried out by adding CIB to the tube containing the intact chloroplasts, followed by centrifugation at 1700 ×g for 3 min (4 °C). Upon centrifugation, chloroplast pellets were resuspended in 500 μL of CIB prior to storage at −30 °C.

2.3. Protein extraction

Extraction of the chloroplast proteins was carried out according to Shiraya et al. [13]. Stored chloroplast pellets were transferred to clean tubes containing an extraction buffer [8 M urea, 2 M thiourea, 244 mM CHAPS, 1 M Tris-HCl (pH 8), 50% (v/v) glycerol, 20% (v/v) Triton X-100 and 1 M DTT]. Then, 15 cycles of 1-min sonication were performed, followed by centrifugation at 3200 ×g for 5 min at 4 °C. The supernatant containing the proteins was collected and transferred to a new tube, and five volumes of cold acetone were then added. Protein precipitation was carried out for 16 h at −30 °C, followed by centrifugation at 3200 ×g for 15 min (4 °C). The protein pellet was finally resuspended in a sample buffer containing 125 mM Tris (pH 6.8), 20% glycerol, 1% SDS and 1% DTT. Protein concentration was estimated by the Bio-Rad Protein Assay kit using bovine serum albumin as the standard.

2.4. Protein identification by GeLC-MS/MS

Aliquots of 25 μg of proteins were separated in 12% SDS-PAGE gels [14], and 5 gel slices were transferred into clean tubes for gel digestion according to Shevchenko et al. [15]. Tryptic peptides were resuspended in 0.1% formic acid in H_2O and separated on a chromatographic system EASY-nLC1000 (Thermo Fisher Scientific) using a C18 nano-column (15 cm, 2 μm, 100 Å) under a constant flow rate of 400 nL min^{-1}. Solvent A consisted of 0.1% formic acid in H_2O, and solvent B was 0.1% formic acid in acetonitrile. The separation gradient was adjusted as follows: 75 min from 100% solvent A to 35% solvent B and 5 min from 35% to 80% solvent B. Ionization and injection of the peptides into the mass spectrometer (Q-Exactive) was carried out through nano-electrospray (nESI) using 3.1 kV applied directly into the injection needle. Mass spectrometry was used with the data-dependent acquisition method for the ten most abundant peptide ions. Full scans and data-dependent scans were acquired with a resolution equal to 70,000 and 35,000 FWHM (full width at half maximum), respectively. Fragment spectra were acquired upon HCD (high-energy collision dissociation) fragmentation of the isolated peptide ions under a normalized collision energy of 25. Peptide ions selected for fragmentation were excluded from a new isolation event for 30 s.

Protein identification was performed through stringent database searches against the *Eucalyptus grandis* protein database, version 1.1 (http://www.phytozome.net/). Spectral correlations were performed by the Sequest, Sequest HT and MS-Amanda search tools embedded in Proteome Discoverer 1.4 using the following search parameters: 20 ppm tolerance for precursor ions and 0.02 Da for fragment ions. Oxidation of methionines and carbamidomethylation of cysteines were selected as dynamic and static modifications, respectively. Peptide-spectrum matches (PSMs) were considered significant if they had a cross-correlation score equal to or higher than 1.5, 2.0 or 2.5 for singly, doubly or triply-charged ions, respectively, for the Sequest and Sequest HT search engines; and, a PSM score equal to or higher than 100 as suggested by the MS-Amanda tool. The false-discovery rate was also adjusted for 1%. Protein descriptions were obtained from the *E. grandis* predicted gene annotations, which are available at the Phytozome website, and the KEGG (http://www.genome.jp/kegg/kegg2.html) pathway 00710 was used to map the proteins and enzymes involved in carbon fixation.

2.5. Estimation of protein relative abundances

Peptide-spectrum matches for each identified protein were normalized according to the NSAF criteria [16]. Statistical analyses were performed in Inferno RDN 1.1.5. When necessary, missing value imputation was carried out by using the NSAF mean of the biological sample. Changes in the abundance of photosynthetic-related enzymes were evaluated by adding the individual NSAF values of each gene product and were considered significant if the *p*-value was below 0.05 according to the Kruskal-Wallis test.

2.6. Assessment of stomatal aperture

Leaf sections of approximately 1 cm^2 were transferred to a 0.1 M potassium phosphate buffer (pH 7.4) containing 3% glutaraldehyde and stored for two days at 4 °C. Fixation of the plant material was carried out by immersion in a solution containing 1% osmium tetroxide and dehydration in a graded ethanol series (from 30% to 100%). After drying (CO_2 at 38 °C and 1200 psi), samples were gold-covered (± 30 nm thickness) and visualized in the scanning electron microscope JSM 5410 (JEOL) with accelerating voltage at 15 kV (500× magnified). The

number of open stomata (width > 1 μm) and the opening degree were measured using Image J 1.48.

2.7. Efficiency of the photosystem II

Leaf chlorophyll fluorescence was determined using a chlorophyll fluorometer OS-30p (Opti-Sciences). Data were acquired after 30 min of dark adaptation from two distinct points in the adaxial leaf surface of the replicates for each treatment. Maximum (F_m) and minimum (F_0) fluorescence values were used for the calculation of the maximum efficiency of PSII [(Fm-Fo)/Fm]. Significant differences were only considered according to Student's t-test at 5% confidence.

2.8. Leaf anatomy

Preparation of leaf samples comprised the following steps: fixation, dehydration, inclusion (using paraffin), sectioning and assembly of the cuts as described in [17]. Toluidine blue tissue staining and deparaffinization were carried out following the protocol described in [18]. To evaluate the integrity and anatomical changes imposed by the CO_2 treatment, the width of the palisade/spongy parenchyma and the upper/lower epidermis were measured. Additionally, width and length of the vascular bundles were also measured using Image J 1.48. Statistical analyses were carried out by Assistat 7.7, and differences were considered significant if the p-value was below 0.05 according to the Mann-Whitney U test.

3. Results and discussion

3.1. Eucalyptus urophylla growth under high CO_2 concentrations induces stomatal closure and changes in leaf anatomy

Carbon dioxide is a key substrate in plant photosynthesis; however, depending on the intensity and duration, a common phenotypic response to high CO_2 stimulus is stomatal closure [19–21]. This phenomenon is triggered by complex signalling processes that occur in guard cells and mesophyll, involving induction and inter-molecular communication between different metabolites such as abscisic acid (ABA), reactive oxygen species (ROS), calcium and protein kinases. Leaves of *Eucalyptus urophylla* showed differences in the number of open stomata and the degree of openness upon CO_2 stimulus (Fig. 1). It was observed that plants grown in the CO_2-enriched atmosphere (1000 ppm) showed a lower number of opened stomata and reduced stomatal pore width. Stomatal closure is a complex process induced by plant growth
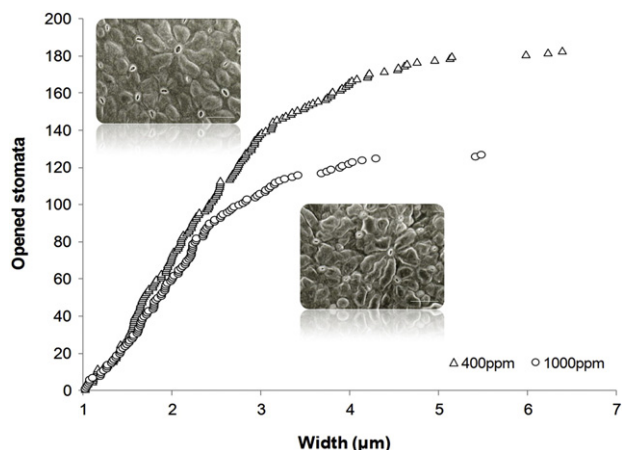
regulators (i.e., ABA) and secondary intracellular messengers, such as Ca^{2+}, K^+ and nitric oxide [23]. Induction of changes in stomatal aperture, as observed in the *E. urophylla* leaves, has already been reported for other plant species grown under high atmospheric CO_2 [19–20,24] and is probably related to control of the diffusion of this photosynthetic substrate into the mesophyll cells. Maximum efficiency of the photosystem II did not significantly change after growth at high CO_2 concentrations for 10 weeks, corroborating the hypothesis of upstream control imposed by the stomatal morphology (Fig. 1S). Little is known about the molecular components involved in the intracellular signalling pathways by which CO_2 controls stomatal development and function. However, our experiment suggests an induction of stomatal closure as a physiological response to the environmental stimulus in *E. urophylla* plants grown at a high CO_2 concentration.

In order to gain insight into other structural changes induced by growth under high CO_2 concentrations, we investigated the *E. urophylla* leaf anatomy from plants grown at 400 and 1000 ppm (Fig. 2). The significant reduction in the length and width of vascular bundles in plants cultivated in the CO_2-enriched atmosphere suggests reduced cell growth and proliferation within this region. Our data contrast with those observed in some *Pinus* species, as an increase in the vascular tissue area has been reported in plant leaves of *P. taeda* [25], *P. radiata* [26] and *P. ponderosa* [27] grown at elevated CO_2 concentrations. In *Pinus palustris* species, a reduction in the phloem area in needles was observed when this species was grown at an elevated CO_2 concentration [28]; on the other hand, in *Populus*, no effect on the palisade and spongy mesophylls was detected upon plant growth at high CO_2 levels [29]. The divergences regarding alterations to the leaf histology imposed by growth at high CO_2 concentrations in woody plants hamper general statements and inter-species correlations because the phenotypic responses depend on the intensity/duration of the stimulus and the genome background of the studied organism. From our data, it is clear that the 1000 ppm CO_2 stimulus induced changes in the leaf anatomy of *E. urophylla* and that the intermediate regulators of this response deserve further investigation.

3.2. Enrichment of chloroplastic proteins enabled identification of the core Calvin-Benson-Bassham cycle enzymes

Acquisition of mass spectrometric data is still mainly achieved through data-dependent approaches that specifically select and isolate the most abundant ions from a survey scan for the fragmentation and
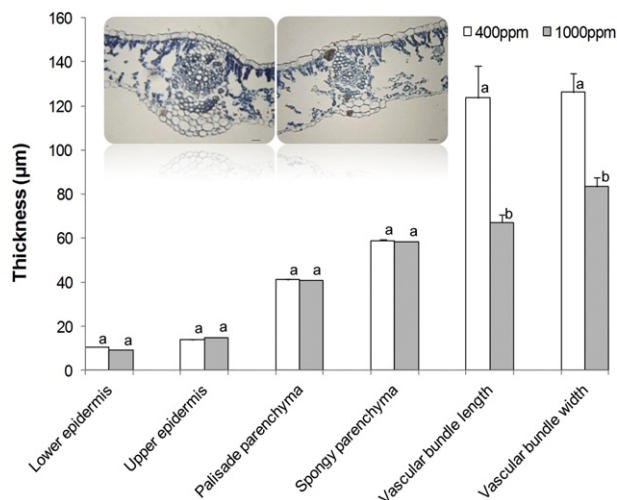

Fig. 1. Scanning electron microscopy of *E. urophylla* leaves cultivated for 10 weeks under a controlled CO_2 atmosphere. Stomata were considered opened if the pore aperture width was >1 μm. Upper right panel: stomata from plants cultivated at a CO_2 concentration adjusted to 400 ppm. Lower left panel: stomata from plants cultivated at a CO_2 concentration adjusted to 1000 ppm. Bar = 50 μm.

Fig. 2. Leaf anatomy analysis of *E. urophylla* plants cultivated for 10 weeks under a controlled CO_2 atmosphere. The results of bright-field microscopy of the midrib vascular bundle from plants cultivated at a CO_2 concentration adjusted to 400 (left) and 1000 (right) ppm are shown in the upper panel. Bar = 20 μm. Different letters denote significant difference according to the Mann-Whitney U test; $p < 0.05$.

generation of fragment mass spectra used in peptide identification. Thus, enrichment strategies adopted with the goal of increasing the concentration of the proteins of interest (e.g., from a particular metabolic pathway) may increase the sensitivity and reproducibility of the acquired data. In the present study, we chose two proteins involved in photosynthesis metabolism as controls to monitor the enrichment process. Additionally, we decided to evaluate (using the NSAF criteria) the change in the quantity of naturally abundant proteins; one could expect a minimal effect of enrichment procedures in these macro-molecules compared to those with lower abundance. Although the photosynthetic-related enzymes are among the most abundant proteins in a plant leaf proteome, chloroplast isolation from *E. urophylla* leaves resulted in the enrichment of both control proteins. Light-harvesting complex II-*B*1 protein (Eucgr. E02381.1) and a RuBisCO small subunit (Eucgr.B03013.1) presented 2.4-fold and 10.5-fold increases in abundance, respectively, as measured by NSAF criteria (Fig. 3). The enrichment procedure adopted here also increased the reproducibility across biological samples in both protein controls, especially for the CBB enzyme that was chosen as a control and that was found in only one replicate in a non-enriched protein sample.

The chloroplast proteome isolated here from *E. urophylla* leaves comprised a total of 816 different proteins (Table 1S and Fig. 2S) and presented a dynamic range spanning approximately four orders of magnitude (Fig. 4). This wide and dynamic range suggests that for every single copy of the least-abundant protein we detected, there are 4000 copies of the most abundant isolated protein: light-harvesting complex II-*B*1 (Eucgr.E02381.1). All 11 core enzymes involved in carbon assimilation were confidently identified and quantified using the chloroplastic enrichment approach described previously. From the 46 predicted gene products, our strategy allowed the identification of 30 protein species directly involved in carbon assimilation (Fig. 4). The proteins with the highest number of isoforms were RuBisCO, glyceraldehyde 3-phosphate dehydrogenase (GAPDH) and fructose bisphosphate aldolase (FBA), from which four, five and six different protein species were identified using the *E. grandis* genome as a reference for database searches. It is important to mention that the only gene product from the enzyme sedoheptulose-bisphosphatase (SBPase, Eucgr.J00242.1) was confidently identified by our mass spectrometry coupled with a homology database search strategy. Our data suggest that mass spectrometric data acquired upon isolation and enrichment procedures could be used for spectral count quantitative analysis, especially to study changes in the abundance of CBB-related enzymes; this label-free
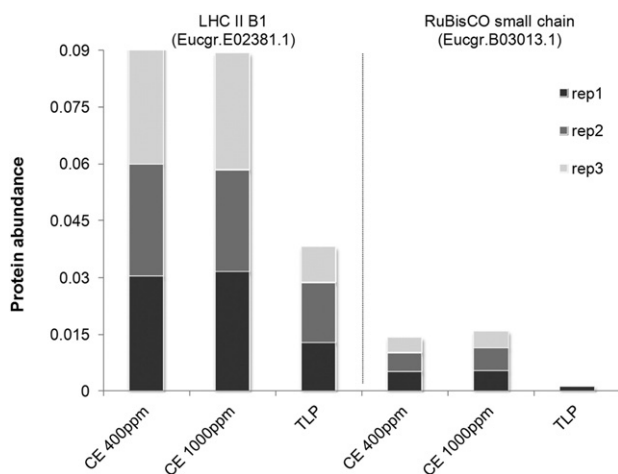

Fig. 4. Dynamic range of the chloroplast proteome isolated from young *E. urophylla* plants. The Calvin-Benson-Bassham cycle enzymes identified in the present study are highlighted. The protein abundance is presented in terms of NSAF and is –Log10 transformed.

quantitative approach largely depends on an unbiased and deep sampling to overcome issues associated with proteins in low abundance that usually generate data with poor reproducibility.

3.3. Eucalyptus urophylla CBB cycle enzymes show a slight but significant increase in abundance upon CO₂ stimulus

Mass spectrometry analysis coupled with stringent database searches against the *E. grandis* translated genome resulted in the identification of all eleven CBB cycle enzymes (Figs. 4, 5). Proteins involved in carbon assimilation are located in the chloroplast stroma, and as long as plastid rupture is efficiently carried out, proteins involved in carbon fixation, regeneration of ribulose-1,5-bisphosphate (RubP) and reduction of 3-phosphoglycerate are easily solubilized and available for MS quantification. In the present work, we identified a slight but significant increase in six of the eleven identified enzymes involved in the cycle (Fig. 5): phosphoglycerate kinase (PGK), glyceraldehyde 3-phosphate dehydrogenase (GAPDH), fructose-bisphosphate aldolase (FBA), fructose-1,6-bisphosphatase (FBPase), sedoheptulose-1,7-bisphosphatase (SBPase) and ribulose-5-phosphate isomerase (RPI) (Fig. 6).

Phosphoglycerate kinase is an enzyme involved in the reversible transfer of phosphate from ATP to 3-P-glycerate, producing 1,3-bisphosphoglycerate, while GAPDH is a key enzyme for catalysing the conversion of 1,3-bisphosphoglycerate (1,3BPG) to glyceraldehyde-3-phosphate (G3P) using ATP and NADPH. Because GAPDH may have a dual metabolic role, acting as an NADPH electron scavenger to protect PS II from ROS-induced damage or as carbon sink player driving carbon assimilation to sucrose and starch synthesis [30–31], GAPDH regulation is crucial for the global balance of the photosynthetic process. In the present work, we identified the enzyme starch synthase (Eucgr.E01068.1) only in plants grown in a CO₂-enriched atmosphere in all three biological replicates, suggesting that starch accumulation is higher in *E. urograndis* plants grown in this condition. It seems that an induction of starch biosynthesis is a common strategy for plants exposed to stress such as cold [32], salinity [33] and heavy metal accumulation [34]. However, the precise function of a higher accumulation of starch under high CO₂ concentrations is still not clear.

Fructose-bisphosphate aldolase is an enzyme involved in the regeneration phase of the CBB cycle. It has been previously shown that this reversible enzyme has a major impact on carbon flux and that the acclimation of photosynthesis to changing environmental conditions (light and CO₂ stimulus) includes and requires changes in plastidic aldolase activity [35–36]. High plastid FBA activity induced RuBP

Fig. 3. Evaluation of *E. urophylla* chloroplast proteome enrichment. Protein abundance is shown in terms of NSAF. CE 400 ppm: Chloroplast-enriched samples from plants grown at a CO₂ concentration adjusted to 400 ppm; CE 1000 ppm: Chloroplast-enriched samples from plants grown at a CO₂ concentration adjusted to 1000 ppm; TLP, total leaf proteome; rep1, biological replicate 1; rep2, biological replicate 2; rep3, biological replicate 3.
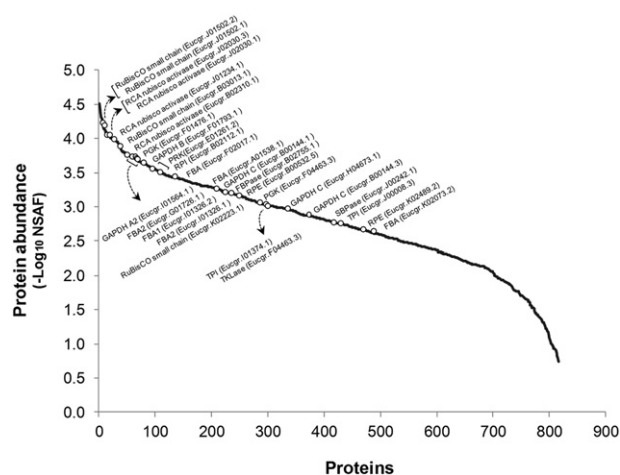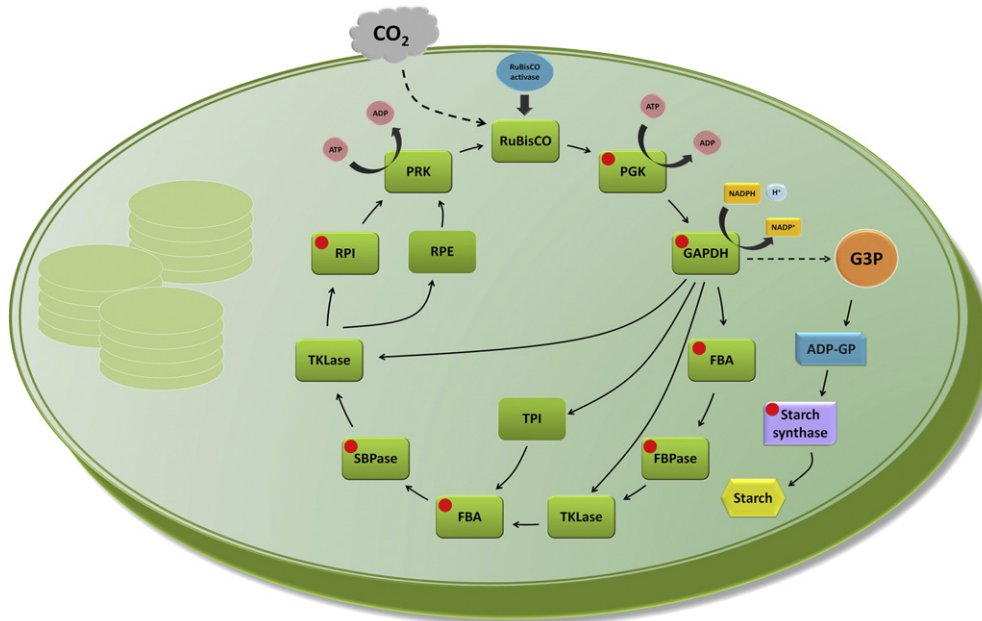
Fig. 5. Schematic presentation of carbon fixation in *E. urophylla* grown under a CO_2– enriched atmosphere. Red dots represent proteins with increased abundance according to the Kruskal-Wallis test; $p < 0.05$.

regeneration and resulted in increased photosynthetic capacity, growth rate, and biomass yield [37]. The enzyme SBPase (Eucgr.J00242.1), which is also involved in the Calvin regeneration phase, was only identified when *E. urophylla* plants were subjected to elevated CO_2. It is important to note that the failure to detect this protein does not mean that it was not present in the biological sample. Instead, the enzyme was probably in such low abundance that its detection was hampered during our GeLC-MS/MS approach. In fact, genome sequencing of *E. grandis* indicates the presence of only one gene product for this enzyme, Eucgr.J00242.1, which was also found in our proteomics approach. Enzyme SBPase acts in one of the Calvin-Benson regeneration paths that ultimately leads to the synthesis of RuBP. Photosynthesis has been shown to be sensitive to changes in SBPase levels [38–40]. In addition, the regenerative capacity of RuBP responded linearly to reductions in SBPase activity, leading to a reduction in total biomass accumulation in *anti*-sense SBPase plants [41]. Increased sedoheptulose-1,7-bisphosphatase activity in transgenic tobacco plants stimulated photosynthesis and growth from an early stage in development [42]. Identification of an increase in the abundance of this enzyme in *E. urograndis* plants grown under high CO_2 concentrations strongly suggests higher carbon assimilation in plants subjected to this environmental condition. In agreement with the changes in abundance of the enzymes PGK, GAPDH, FBA, FBPase and SBPase, the enzyme RPI showed an increased abundance in *E. urophylla* plants cultivated under high atmospheric CO_2 concentrations.

Thioredoxins (Trx) are conserved proteins capable of reducing disulfide bonds of target proteins and, as a consequence, modulate its activities [43]. They play an important role in the ROS counter-acting system but are also mainly involved in carbon assimilation control due to their potential regulatory functions in the central RuBP regenerative enzymes FBPase and SBPase. In the present work, we identified 17 Trx isoforms in *E. urophylla* chloroplasts and one isoform with an increased abundance in plants exposed to high CO_2 concentrations, which corroborates our hypothesis of a stimulus of carbon assimilation metabolism in *E. urophylla* plants exposed to high CO_2 concentrations.

4. Conclusions

Using a GeLC-MS/MS approach coupled with a stringent database search against a closely related *Eucalyptus* species, 816 proteins were identified from isolated chloroplasts of *E. urophylla*. Our proteomics approach indicates a positive metabolic response regarding carbon fixation in a CO_2-enriched atmosphere. The slight but significant increase in the abundance of the CBB cycle enzymes suggests that stomatal closure did not prevent an increase in the carbon assimilation rates. Additionally, chloroplast redox status is one of the potential regulatory mechanisms that could play a role downstream in stomatal closure regulation; the detection of an increase in Trx isoforms is evidence of oxidative control of the CBB cycle. The protein identifications and differential regulation provided here contribute to a deeper understanding of the biochemical events of C3-type carbon fixation.

A comprehensive list of all identified proteins (including accession numbers, identified peptides, MS/MS scores and PSMs) can be found in Tables 2S—7S.

Supplementary data to this article can be found online at http://dx.doi.org/10.1016/j.jprot.2016.09.010.
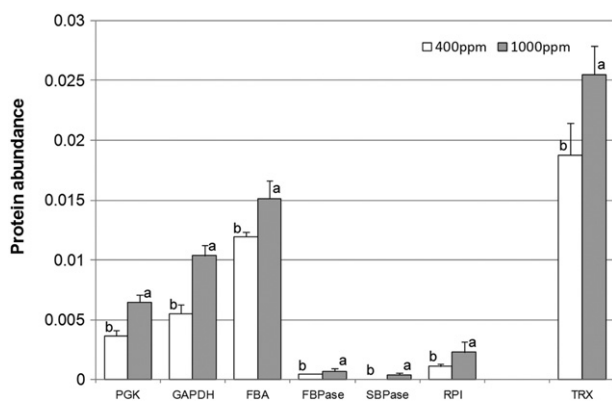

Fig. 6. Calvin-Benson-Bassham cycle proteins are differentially regulated, according to the Kruskal-Wallis test ($p < 0.05$), in *E. urophylla* plants cultivated at a CO_2 concentration adjusted to 1000 ppm in relation to those cultivated at 400 ppm. Values represent the average of three biological replicates ± standard error.

Conflict of interest

The authors declare that they have no conflict of interest.

Acknowledgements

References

[1] Earth System Research Laboratory, National Oceanic and Atmospheric Administration, Trends in Atmospheric Carbon Dioxide, www.esrl.noaa.gov/gmd/ccgg/trends/2016 (Accessed 01.07.2016).

[2] C.D. Keeling, Rewards and penalties of monitoring the earth, Annu. Rev. Energy Environ. 23 (1998) 25–82.

[3] Intergovernmental Panel on Climate Change, in: R.K. Pachauri, L.A. Meyer (Eds.), Climate Change 2014: Synthesis Report. Contribution of Working Groups I, II and III to Fifth Assessment Report of the Intergovernmental Panel on Climate Change, IPCC, Geneva, Switzerland, 2014 (151 pp).

[4] The Arabidopsis Genome Initiative, Analysis of the genome sequence of the flowering plant Arabidopsis thaliana, Nature 408 (2000) 796–815.

[5] A.A. Myburg, D. Grattapaglia, G.A. Tuskan, U. Hellsten, R.D. Hayes, J. Grimwood, J. Jenkins, E. Lindquist, H. Tice, D. Bauer, D.M. Goodstein, I. Dubchak, A. Poliakov, E. Mizrachi, A.R.K. Kullan, S.G. Hussey, D. Pinard, K. van der Merwe, P. Singh, I. van Jaarsveld, O.B. Silva-Junior, R.C. Togawa, M.R. Pappas, D.a. Faria, C.P. Sansaloni, C.D. Petroli, X. Yang, P. Ranjan, T.J. Tschaplinski, C.-Y. Ye, T. Li, L. Sterck, K. Vanneste, F. Murat, M. Soler, H.S. Clemente, N. Saidi, H. Cassan-Wang, C. Dunand, C.A. Hefer, E. Bornberg-Bauer, A.R. Kersting, K. Vining, V. Amarasinghe, M. Ranik, S. Naithani, J. Elser, A.E. Boyd, A. Liston, J.W. Spatafora, P. Dharmwardhana, R. Raja, C. Sullivan, E. Romanel, M. Alves-Ferreira, C. Külheim, W. Foley, V. Carocha, J. Paiva, D. Kudrna, S.H. Brommonschenkel, G. Pasquali, M. Byrne, P. Rigault, J. Tibbits, A. Spokevicius, R.C. Jones, D.A. Steane, R.E. Vaillancourt, B.M. Potts, F. Joubert, K. Barry, G.J. Pappas, S.H. Strauss, P. Jaiswal, J. Grima-Pettenati, J. Salse, Y. Van de Peer, D.S. Rokhsar, J. Schmutz, The genome of Eucalyptus grandis, Nature 509 (2014) 356–362.

[6] J.S. Andersen, M. Mann, Organellar proteomics: turning inventories into insights, EMBO Rep. 7 (2006) 874–879.

[7] A. Pandey, S. Chakraborty, A. Datta, N. Chakraborty, Proteomics approach to identify dehydration responsive nuclear proteins from chickpea (Cicer arietinum L.), Mol. Cell. Proteomics 7 (2008) 88–107.

[8] T. Kleffmann, D. Russenberger, A. Von Zychlinski, W. Christopher, K. Sjalander, W. Gruissem, S. Baginsky, The Arabidopsis thaliana chloroplast proteome reveals pathway abundance and novel protein functions, Curr. Biol. 14 (2004) 354–362.

[9] J. Bauhus, P. van der Meer, M. Kanninen, Ecosystem Goods and Services from Plantation Forests, 2011.

[10] R.J. Luxmoore, S.D. Wullschleger, P.J. Hanson, Forest responses to CO2 enrichment and climate warming, Water Air Soil Pollut. 70 (1993) 309–323.

[11] B.J. Atwell, M.L. Henery, G.S. Rogers, S.P. Seneweera, M. Treadwell, J.P. Conroy, Canopy development and hydraulic function in Eucalyptus tereticornis grown in drought in CO2-enriched atmospheres, Funct. Plant Biol. 34 (2007) 1137–1149.

[12] A.G. Quentin, K.Y. Crous, C.V.M. Barton, D.S. Ellsworth, Photosynthetic enhancement by elevated CO2 depends on seasonal temperatures for warmed and non-warmed Eucalyptus globulus trees, Tree Physiol. 35 (2015) 1249–1263.

[13] T. Shiraya, K. Kaneko, T. Mitsui, Quantitative proteomic analysis of intact plastids, in: J.V. Jorrin-Novo, S. Komatsu, W. Weckwerth, S. Wienkoop (Eds.),Plant Proteomics Methods and Protocols Series: Methods in Molecular Biology 2014, pp. 469–480.

[14] U.K. Laemmli, Cleavage of structural proteins during assembly of head of bacteriophage-T4, Nature 227 (1970) 680–685.

[15] A. Shevchenko, H. Tomas, J. Havlis, J.V. Olsen, M. Mann, In-gel digestion for mass spectrometric characterization of proteins and proteomes, Nat. Protoc. 1 (2006) 2856–2860.

[16] A.C. Paoletti, T.J. Parmely, C. Tomomori-Sato, S. Sato, D. Zhu, R.C. Conaway, J.W. Conaway, L. Florens, M.P. Washburn, Quantitative proteomic analysis of distinct mammalian mediator complexes using normalized spectral abundance factors, Proc. Natl. Acad. Sci. U. S. A. 103 (2006) 18928–18933.

[17] D.A. Johansen, Plant Microtechnique, McGraw-Hill Book Company, Inc, New York, 1940.

[18] W.S. Sakai, Staining Technique, 5, Department of Botany, University of Hawaii, Honolulu, 1973 247–249.

[19] B.G. Drake, M.A. Gonzalez-Meler, S.P. Long, MORE EFFICIENT PLANTS: a consequence of rising atmospheric CO2, Annu. Rev. Plant Physiol. Plant Mol. Biol. 48 (1997) 609–639.

[20] A. Vavasseur, A.S. Raghavendra, Guard cell metabolism and CO2 sensing, New Phytol. 165 (2005) 665–682.

[21] K. Shi, X. Li, H. Zhang, G. Zhang, Y. Liu, X. Xia, Z. Chen, J. Yu, Rapid Report Guard Cell Hydrogen Peroxide and Nitric Oxide Mediate Elevated CO2-Induced Stomatal Movement in Tomato, 2015 342–353.

[23] R. Desikan, R. Griffiths, J. Hancock, S. Neill, A new role for an old enzyme: nitrate reductase-mediated nitric oxide generation is required for abscisic acid-induced stomatal closure in Arabidopsis thaliana, Proc. Natl. Acad. Sci. U. S. A. 99 (2002) 16314–16318.

[24] T.-H. Kim, M. Bohmer, H. Hu, N. Nishimura, J.I. Schroeder, Guard cells signal transduction network: advances in understanding abscisic acid CO2, and Ca2 + signalling, Annu. Rev. Plant Biol. 61 (2010) 561–591.

[25] J.F. Thomas, C.H. Harvey, Leaf anatomy of four species grown under continuous CO2 enrichment, Bot. Gaz. 144 (1983) 303–309.

[26] J. Conroy, E.W.R Barlow, D.I. Bevege, Response of Pinus radiata seedlings to carbon dioxide enrichment at different levels of water and phosphorus: growth, morphology and anatomy, Ann. Bot. 57 (1986) 165–177.

[27] J.C. Pushnik, R.S. Demaree, J.L.J. Houpis, W.B. Flory, S.M. Bauer, P.D. Anderson, The effect of elevated carbon dioxide on a Sierra-Nevadan dominant species: Pinus ponderosa, J. Biogeogr. 22 (1995) 249–254.

[28] S.G. Pritchard, C.M. Peterson, S.A. Prior, H.H. Roger, Elevated atmospheric CO2 differentially affects needle chloroplast ultrastructure and phloem anatomy in Pinus palustris: interactions with soil resource availability, Plant Cell Environ. 20 (1997) 461–471.

[29] K.M. Radoglou, P.G. Jarvis, Effects of CO2 enrichment on four poplar clones: growth and leaf anatomy, Ann. Bot. 65 (1990) 617–626.

[30] X. Wang, L. Chang, B. Wang, D. Wang, P. Li, L. Wang, X. Yi, Q. Huang, M. Peng, A. Guo, Comparative proteomics of Thellungiella halophila leaves from plants subjected to salinity reveals the importance of chloroplastic starch and soluble sugars in halophyte salt tolerance, Mol. Cell. Proteomics 12 (2013) 2174–2195.

[31] L. Chang, A. Guo, X. Jin, Q. Yang, D. Wang, Y. Sun, Q. Huang, L. Wang, C. Peng, X. Wang, The beta subunit of glyceraldehyde 3-phosphate dehydrogenase is an important factor for maintaining photosynthesis and plant development under salt stress—based on an integrative analysis of the structural, physiological and proteomic changes in chloroplasts, Plant Sci. 236 (2015) 223–238.

[32] X. Peng, L. Teng, X. Yan, M. Zhao, S. Shen, The cold responsive mechanism of the paper mulberry: decreased photosynthesis capacity and increased starch accumulation, BMC Genomics 16 (2015) 898.

[33] K.S. Sree, K. Adelmann, C. Garcia, E. Lam, K.-J. Appenroth, Natural variance in salt tolerance and induction of starch accumulation in duckweeds, Planta 241 (2015) 1395–1404.

[34] K. Higuchi, M. Kanai, M. Tsuchiya, H. Ishii, N. Shibuya, N. Fujita, Y. Nakamura, N. Suzui, S. Fujimaki, E. Miwa, Common reed accumulates starch in its stem by metabolic adaptation under Cd stress conditions, Front. Plant Sci. 6 (2015) 1–6.

[35] V. Haake, R. Zrenner, U. Sonnewald, M. Stitt, A moderate decrease of plastid aldolase activity inhibits photosynthesis, alters the levels of sugars and starch, and inhibits growth of potato plants, Plant J. 14 (1998) 147–157.

[36] V. Haake, M. Geiger, P. Walch-Liu, C. Engels, R. Zrenner, M. Stitt, Changes in aldolase activity in wild-type potato plants are important for acclimation to growth irradiance and carbon dioxide concentration, because plastid aldolase exerts control over the ambient rate of photosynthesis across a range of growth conditions, Plant J. 17 (1999) 479–489.

[37] K. Uematsu, N. Suzuki, T. Iwamae, M. Inui, H. Yukawa, Increased fructose 1,6-bisphosphate aldolase in plastids enhances growth and photosynthesis of tobacco plants, J. Exp. Bot. 63 (2012) 3001–3009.

[38] E.P. Harrison, N.M. Willingham, J.C. Lloyd, C.A. Raines, Reduced sedoheptulose-1,7-bisphosphatase levels in transgenic tobacco lead to decreased photosynthetic capacity and altered carbohydrate accumulation, Planta 204 (1998) 27–36.

[39] C.A. Raines, E.P. Harrison, H. Olcer, J.C. Lloyd, Investigating the role of the thiol-regulated enzyme sedoheptulose-1,7-bisphosphatase in the control of photosynthesis, Physiol. Plant. 110 (2000) 303–308.

[40] H. Olçer, J.C. Lloyd, C.A. Raines, Photosynthetic capacity is differentially affected by reductions in sedoheptulose-1,7-bisphosphatase activity during leaf development in transgenic tobacco plants, Plant Physiol. 125 (2001) 982–989.

[41] E.P. Harrison, Small decreases in SBPase cause a linear decline in the apparent RuBP regeneration rate, but do not affect Rubisco carboxylation capacity, J. Exp. Bot. 52 (2001) 1779–1784.

[42] S. Lefebvre, T. Lawson, M. Fryer, O.V. Zakhleniuk, J.C. Lloyd, C.A. Raines, Increased sedoheptulose-1, 7-bisphosphatase activity in transgenic tobacco plants stimulates photosynthesis and growth from an early stage in development, Plant Physiol. 138 (2005) 451–460.

[43] K. Motohashi, Y. Okegawa, Method for enhancement of plant redox-related protein expression and its application for in vitro reduction of chloroplastic thioredoxins, Protein Expr. Purif. 101 (2014) 1–6.